THE AMERICAN MINERALOGIST, VOL. 47, MAY–JUNE, 1962

PBC VECTOR, CRITICAL BOND ENERGY RATIO AND CRYSTAL EQUILIBRIUM FORM

G. A. WOLFF[1] AND J. G. GUALTIERI, *U. S. Army Signal Research and Development Agency Fort Monmouth, New Jersey.*

ABSTRACT

The various methods of deriving crystal equilibrium forms are reviewed. Crystal habit and microcleavage are presented in terms of specific surface energy, PBC vectors and two-dimensional nucleation. The influence of hemihedrism on the specific surface energy is discussed. For compounds or elements having bonds of different strengths, the concept of a critical bonding ratio is introduced, and its value shown to be readily determined. The role of adsorption and of departures from ideal surface structure is demonstrated.

INTRODUCTION

The idea that crystal habit is closely related to the internal structure of the crystal was first expressed by A. Bravais, who emphasized the importance of crystal planes of high reticular density. Along this line, Donnay and Harker (1937) later demonstrated the influence of screw axes and glide planes on crystal habit. Wells (1946) and Buerger (1947) also dealt with this subject. The significance of the atomic array in determining crystal habit was then shown by Kossel (1928), Stranski (1928), Hartman (1958), Kern *et al.* (1956) and Kleber (1937). Stranski and others later estimated the influence of departures from the ideal surface structure (Stranski and Honigmann, 1950) and of adsorption (Stranski, 1956; Kleber, 1957; Hartman, 1959) on crystal morphology. There also have been several attempts at correlating crystal habit with surface free energy and its plot in spherical coordinates (Wulff's plot or "γ plot" (Wulff, 1901; Yamada, 1924; Herring, 1950)). This approach appears desirable to the authors since it permits generalizations and predictions to be made with regard to the theoretical growth, or cleavage habit. It is demonstrated herein that differences between experimental and derived habits yield specific information with regard to the nature of adsorption, surface lattice deformation, and the character of bonding, both in the bulk and at the surface of crystals. The special role of microcleavage habit (Wolff and Broder, 1959) is also discussed. A correlation of Wulff's plot, PBC (Periodic Bond Chain) vectors (Hartman and Perdok, 1955) crystal habit, microcleavage and activation energy of two-dimensional nucleation will be presented. In addition, the relation of Wulff's plot to Stranski's method (Stranski, 1928) of determining equilibrium forms is shown. The development of crystal habits differing from the theoretically derived equilibrium forms can be explained through the establishment of

[1] Present address: The Harshaw Chemical Company, Solid State Research Laboratory, 2240 Prospect Avenue, Cleveland 15, Ohio.

new PBC vestors; the latter result from atomic displacements (Stranski and Honigmann, 1950; Wolff and Broder, 1959; Wolff, 1962) in the surface or through the adsorption of foreigh atoms.

The utilization of the PBC vector as introduced by Hartman and Perdok (1955) greatly facilitates the understanding of the equilibrium form of crystals and its derivation from the crystal structure. A periodic bond chain in a crystal plane is an array of atoms or crystal building blocks which are held together by bonds. In each array every atom, or building block, is bonded more strongly to the crystal than the atom or building block in the equilibrium position on the crystal surface; or, expressed in a different way, the detachment energy of each atom, or building block, is greater than the average or mean detachment energy of the atoms or building blocks of the surface layer when they are detached from the crystal one by one. In this way, the periodic bond chains are easily determined for simple crystal structures. For complicated structures an unambiguous and easy way for their determination is by the calculation of Wulff's surface energy plot as shown in this paper. The periodic bond chains are identical to the directions of the "surface energy valleys" of this plot. The PBC vectors denote the direction and magnitude of the full translation distance of the periodic bond chains.

Formulae of Gibbs and Wulff

Gibbs (1928) found that a crystal is in equilibrium with its own vapor phase when for constant volume, its total surface energy is a minimum.

$$\sum_i \sigma_i A_i = \sigma_1 A_1 + \sigma_2 A_2 + \cdots \sigma_n A_n = \text{minimum} \tag{1}$$

σ_i = specific free surface energy of the ith crystal plane.
A_i = area of the ith crystal plane.

Wulff (1901) showed that this statement is equivalent to the equation

$$\frac{\sigma_1}{h_1} = \frac{\sigma_2}{h_2} = \frac{\sigma_3}{h_3} \cdots \frac{\sigma_n}{h_n} = \frac{\sigma_i}{h_i} = \text{constant} \tag{2}$$

where h_i = central distance of the i^{th} crystal plane.

It is implicit in Gibbs' original formula (not given here) that a crystal will assume the equilibrium form only when it is of microscopic dimensions. Polyhedral macroscopic crystals are, in all probability, not equilibrium forms but growth forms. Whereas the boundary planes of the former are determined by their specific surface free energies, the boundary planes of the latter result from slow growth in the normal direction which, in turn, is induced by the presence of a two-dimensional nucleation energy. According to Stranski and Kaishev, (1935) these planes are the same as the planes that belong to the equilibrium form. This does not

mean, however, that the growth form is identical with the equilibrium form, since the relative sizes of the various planes usually differ in the two forms. In a limited way, this consideration holds true also for imperfect crystals which grow via screw dislocations. Their growth rate is largely determined by the activation energy of the one-dimensional nucleation.

Practical Derivation of Equilibrium Forms

A crystal equilibrium form may be derived in two ways:

1. The first method consists of varying the central distance of all crystal planes until they are proportional to the specific surface free energy (Wulff's method) (Stranski, 1956). This construction follows from eq. (2). In a first approximation, the specific surface free energy may be replaced by the specific surface free energy at 0° K, *i.e.*, the specific surface energy.
2. In the second method, one removes from a crystal model all "building blocks" that are bonded less strongly than those in the semicrystalline position, *i.e.*, growth position (Stranski, 1928). As an example, should the evaporation probability of a "building block" occupying a corner position be greater than that in a semicrystalline position, the corner "building block" will evaporate and leave the position vacant. In a like manner, neighboring loosely bound "building blocks" will evaporate and a new plane will appear. The resulting form, the equilibrium form, will contain "building blocks" whose evaporation probability is less than or equal to that of the semicrystalline position.

The specific surface energy σ_i is defined as being half the energy per unit area required to separate the crystal along the i^{th} plane. This results from the fact that two surfaces are created and only half the energy of separation per surface need to be considered. This is correct, however, only when both surfaces are identical. For Van der Waals, metallic and covalent bonding where the interaction energy decreases with interatomic distance; the separation energy increases with the number of atoms at first, second or higher nearest neighbor distances which are separated from their respective neighbors during the process. Consequently, σ_i will be equal to half the sum of the products $\Sigma_j N_j E_j$ of the number of different neighbors (N_1, N_2, N_3 . . . etc.) involved in the separation process and their energy of interaction (E_1, E_2, E_3 . . . etc.) per unit area of the i^{th} plane.

In two dimensions, Wulff's construction is a polar diagram of the specific surface energies of the various planes which belong to a particular zone. (Fig. 5 and 6). The crystal form which corresponds to the lowest surface energy may be obtained by selecting the planes enclosing the

smallest area. The respective planes are orthogonal to lines drawn from the origin and intersect these lines at distances proportional to the specific surface energy of the specific plane.

In a three-dimensional representation, the specific surface energies σ_i of all planes are plotted in spherical coordinates (Fig. 1). Equations for σ_i may then be derived in terms of crystalllgraphic indices hkl. Once these equations are determined for a sufficient number of planes, the areas can be found in spherical space where the equations hold for all planes. These areas are bounded by crystallographic zones of low surface energy which form spherical polygons. Each of the areas has one maximum (σ_{max}) representing the antipole of a sphere with the pole passing through the origin (Wulff's point, or center) of the crystal. The surface energy diagram of the boundary zones, or "valleys," are intersections of two such spheres. The intersections of "valleys" are known as "cusps." Hence, "cusps," "valleys," and "maxima" in a Wulff's diagram correspond respectively to "planes," "edges," and "corners" in an equilibrium form (Fig. 1).

For any type of bonding, such as nearest neighbor bonding, it can be shown that the ratio

$$\sigma_i/\sigma_{max} = \cos \delta$$

where δ is the angle between the i^{th} plane vector and the maximum plane vector. This is equivalent to: (See Figure 2)

$$\vec{\sigma}_i(\vec{\sigma}_i - \vec{\sigma}_{max}) = 0 \tag{3}$$

or

$$\sigma_i(\sigma_i - \sigma_{max} \cos (\vec{\sigma}_i, \vec{\sigma}_{max})) = 0 \tag{4}$$

with

$$\vec{\sigma}_i = u_i\vec{a} + v_i\vec{b} + w_i\vec{c} \tag{5}$$

and

$$\vec{\sigma}_{max} = u_{max}\vec{a} + v_{max}\vec{b} + w_{max}\vec{c} \tag{6}$$

and since

$$\cos (\vec{\sigma}_i, \vec{\sigma}_{max}) = \cos (\vec{\sigma}_i{}^*, \vec{\sigma}_{max}) = \frac{\vec{\sigma}_{max} \cdot \vec{\sigma}_i{}^*}{\sigma_{max} \cdot \sigma_i{}^*}, \tag{7}$$

substitution yields

$$\sigma_i = \frac{\vec{\sigma}_i{}^* \cdot \vec{\sigma}_{max}}{\sigma_i{}^*}. \tag{8}$$

Defining

$$\sigma_i = \sigma_{hkl}$$

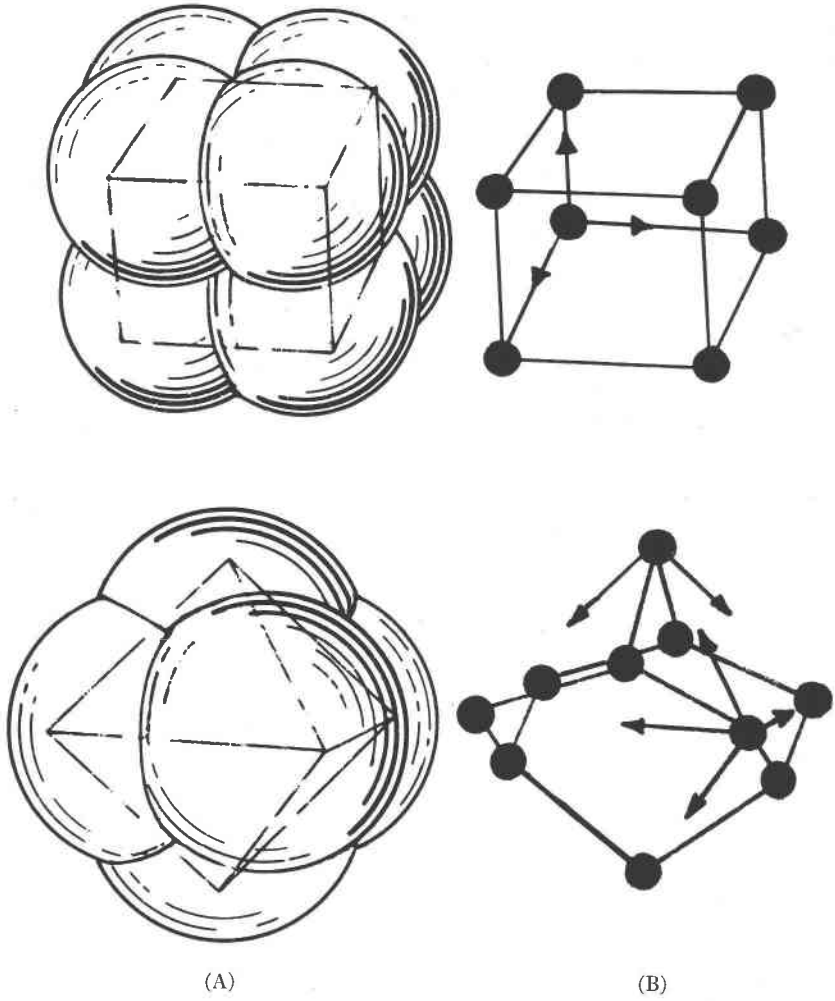

(A) (B)

FIG. 1 A) Surface free energy plot of a crystal of simple cubic structure in spherical coordinates. Only nearest neighbor interaction is taken into account. Each cusp corresponds to an equilibrium plane (001); each valley connecting the cusps correspondingly represents an edge. This edge is [100] and is the common boundary to two adjacent (001) planes. The valleys are "complete," *i.e.* they can be traced 360° from cusp to cusp around the plot along one zone. A complete valley corresponds to a straight array of atoms. The equilibrium form (001) is inscribed.

B) Surface free energy plot for a crystal of diamond structure in spherical coordinates. Only nearest neighbor interaction is taken into account. The cusps correspond to (111) planes and the valleys connecting them correspond to [011] edges which are common to two neighboring (111) planes. The valleys are "incomplete," *i.e.* they cannot be traced 360° around the plot. An incomplete valley corresponds to a zig-zag array. The equilibrium form (111) is inscribed. The corresponding PBC vectors are given at the right.

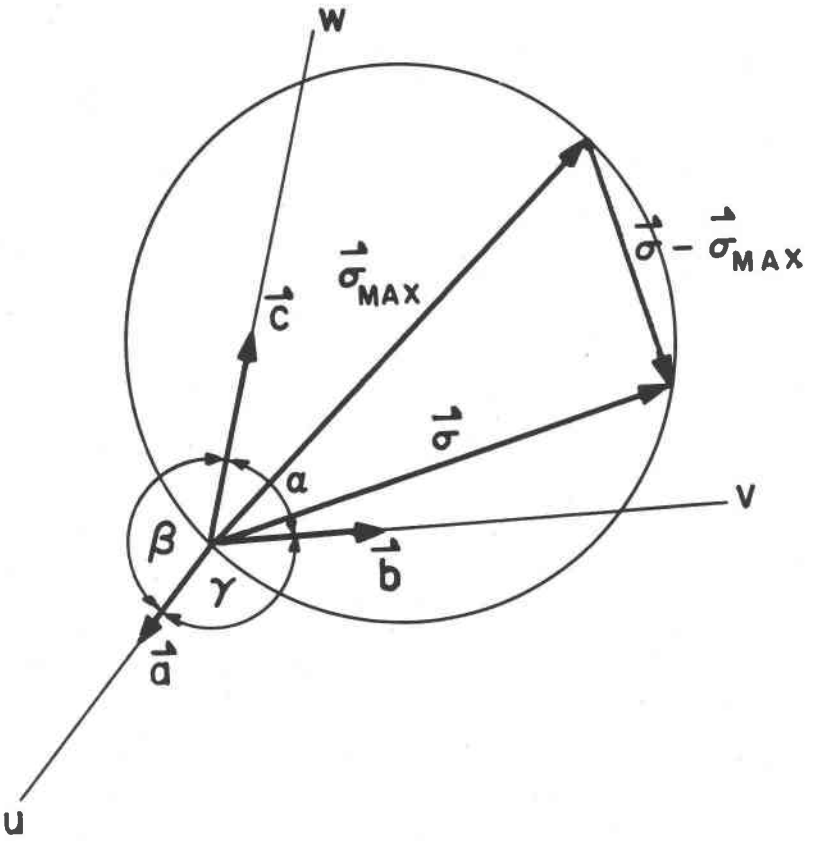

FIG. 2. Vector representation of surface energy. $\vec{\sigma}$max = maximum point in Wulff's plot. $\vec{\sigma}$ = surface energy of any plane.

and its respective vector in reciprocal space

$$\vec{\sigma}_i^* = h_i\vec{a}^* + k_i\vec{b}^* + l_i\vec{c}^*,$$

we then have

$$\sigma_{hkl} = (u_{max}h_i + v_{max}k_i + w_{max}l_i)/(h^2b^2c^2 \sin^2\alpha + k^2c^2a^2 \sin^2\beta + l^2a^2b^2 \sin^2\gamma + 2klbca^2(\cos\beta \cos\gamma - \cos\alpha) + 2lhcab^2(\cos\gamma \cos\alpha - \cos\beta) + 2hkabc^2(\cos\alpha \cos\beta - \cos\gamma))^{1/2}. \quad (9)$$

σ_{max} can be derived by simply summing all PBC vectors of the unit cell which form an angle of less than 90° with any vector within a spherical polygon. For example, [001]+[010]+[100]=[111] for the spherical triangle $h, k, l \geq 0$ in simple cubic structure. This holds for structures having linear atomic arrays. For structures having zig zag arrays, only so-called

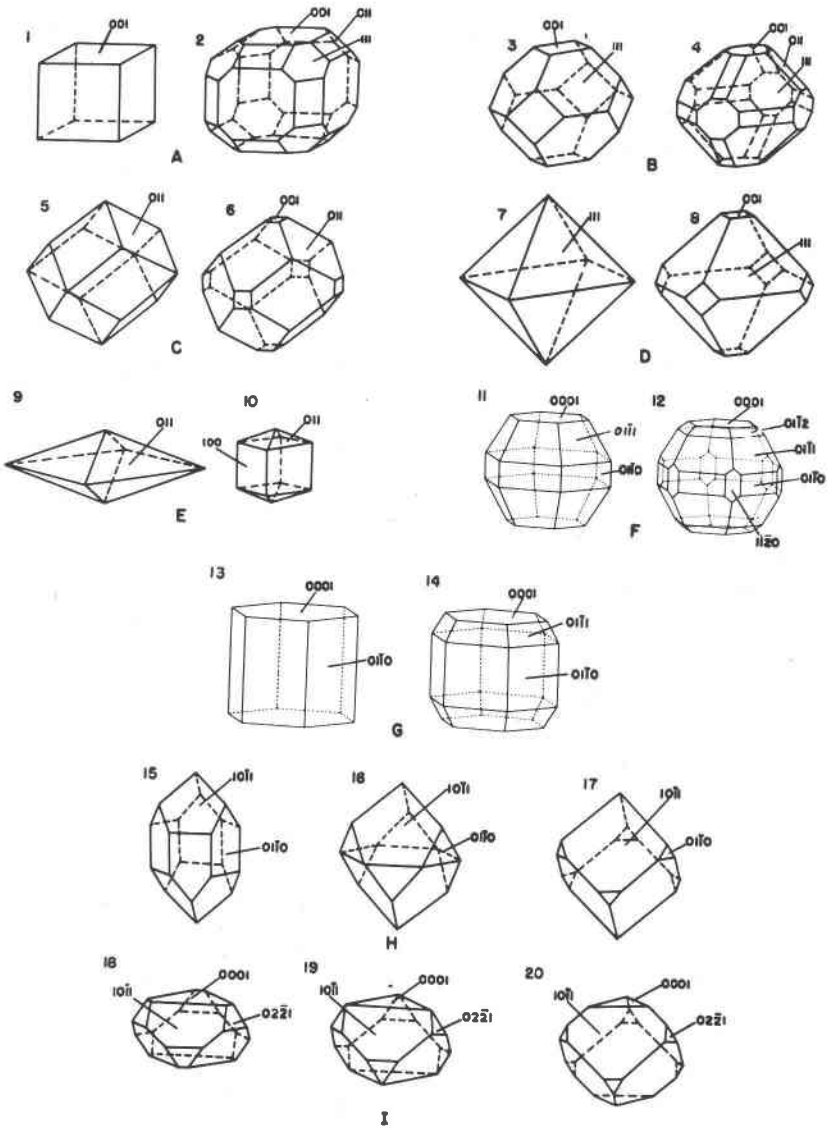

FIG. 3. Nos. 1–20 Three-dimensional drawings of the equilibrium forms in clinographic projection.

1) s.c. as a result of 1st NN interaction only. 2) s.c. 1st and 2nd NN only. 3) f.c.c. 1st. 4) f.c.c. 1st and 2nd. 5) b.c.c. 1st. 6) b.c.c. 1st and 2nd. 7) diamond 1st. 8) diamond 1st and 2nd. 9) β-Sn 1st. 10) β-Sn 1st and 2nd. 11) h.c.p. 1st. 12) h.c.p. 1st and 2nd. 13) wurtzite 1st. 14) wurtzite 1st and 2nd. 15) Se, where $E_\beta < \frac{1}{2}E_\alpha$. 16) Se, $E_\beta = \frac{1}{2}E_\alpha$. 17) Se, $E_\beta > \frac{1}{2}E_\alpha$. 18) As, $E_\beta < \frac{1}{3}E_\alpha$. 19) As, $E_\beta = \frac{1}{3}E_\alpha$. 20) As, $E_\beta > \frac{1}{3}E_\alpha$. (s.c.—simple cubic; f.c.c.—face centered cubic; b.c.c.—body centered cubic; h.c.p.—hexagonal close-packing; NN—nearest neighbor.)

"effective" PBC vectors alone are added. For example, in diamond for the spherical square h, $k \leq l$, σ_{max} is given by

$$2[011] + 2[0\bar{1}1] \quad \text{or} \quad 2[\bar{1}01] + 2[101] = [004]$$

In this case, the prospective vectors [110], [1$\bar{1}$0], [$\bar{1}\bar{1}$0], and [$\bar{1}$10] are not effective PBC vectors since after a separation parallel to these vectors, every atom or molecule becomes separated from as many neighbors as there are in the equilibrium position; that is, from one atom or molecule too many.

As a result, the following three conditions hold: 1) Any plane which truncates a corner of the equilibrium form contains atoms or molecules in the equilibrium position. These may be attached or detached without any activation energy of one- or two-dimensional nucleation "A_0"; *i.e.* one- or two-dimensional nucleation in this plane is not necessary. 2) Any plane parallel to and truncating an edge of the equilibrium form is parallel to one PBC vector and hence has atoms or molecules bonded to one neighbor more than the atom or molecule in the equilibrium position. A one-dimensional nucleation energy "A_1" is a requisite for the growth of such planes[1]. 3) A plane which is parallel to a plane of the equilibrium form is parallel to at least two PBC vectors, and thus contains atoms or molecules that are bound to at least two more neighbors than those atoms or molecules in the equilibrium position. In this type of plane there exists a two-dimensional nucleation energy "A_2"; *i.e.*, these planes grow via two-dimensional nucleation. This holds true mainly for perfect crystals. As a consequence, there exists in crystal equilibrium forms and growth or solution forms only flat A_2 planes of the type mentioned under 3), striated A_1 planes of the type mentioned under 2), or roughened A_0 planes as mentioned under 1). (These terms have been used by Honigmann (1959), and the planes correspond to "K," "S" and "F" planes (kinked, stepped and flat) of Burton and Cabrera (1949).)

It was mentioned earlier that the atoms or molecules in the corner positions of the equilibrium form are attached to as many neighbors as those in the equilibrium position. Consequently these same corner atoms or molecules will be left untouched in Stranski's derivation of the equilibrium form.

The formulae for specific surface energy of the planes of some of the more common structures are listed in Table I. The equilibrium forms which result when only first nearest neighbor interaction is taken into account, or when interaction is considered of first-plus-second nearest neighbors, have been drawn in Fig. 3 in three-dimensional perspective by standard crystallographic techniques. Stereographic plots of the equi-

[1] This result holds true for perfect and imperfect crystals (ideal and real crystals) as well.

TABLE I

Specific energies of common elemental structures. The number of free bonds ("dangling bonds") at the surface are given for 1st, 2nd, 3rd and sometimes 4th nearest neighbor interaction only. For example, for the plane (314) of the simple cubic structure, the corresponding value is

$$\frac{(h+k+l)n_1 + 2(k+2l)n_2 + 4ln_3}{a_0^2(h^2+k^2+l^2)^{1/2}} = \frac{8n_1 + 18n_2 + 16n_3}{a_0^2 26^{1/2}}$$

or

$$\frac{(h+k+l)n_1 + 2(k+2l)n_2 + 2(h+k+l)n_3}{a_0^2(h^2+k^2+l^2)^{1/2}} = \frac{8n + 18n_2 + 16n_3}{a_0^2 26^{1/2}}$$

n_1, n_2, n_3 represent the free bond energies for 1st, 2nd and 3rd nearest neighbor interaction. Since (314) lies at the boundary of the spherical triangle and quadrangle bounded by the planes (011), (101), (110) and (011), (101), (0$\bar{1}$1), ($\bar{1}$01) respectively, both formulae hold true for this plane for 3rd nearest neighbor interaction. It should be noted that "hexagonal diamond structure" is related to wurtzite in the same way as is the(cubic) diamond structure related to sphalerite, *i.e.* if identical atoms are assumed to occupy the sulfur and zinc positions in wurtzite, this results in a "hexagonal diamond" structure.

TABLE I, PART 1

Structure	Nearest Neighbor Interaction	Spherical Polygon	σ_{hkl} Multiplied by $a^2(h^2+k^2+l^2)^{1/2}$	Equilibrium Planes in Order of Their Appearance
simple cubic	1st	(001, 010, 100)	$h+k+l$	
	2nd	(001, 111, 1$\bar{1}$1)	$2(k+2l)$	
	3rd	(011, 101, 0$\bar{1}$1, $\bar{1}$01)	$4l$	
		(101, 110, 011)	$2(h+k+l)$	

*	1st	2nd	3rd
1st	001	011 001	011
2nd		111 001	112 011
3rd			011

* Intersects; *e.g.*, in simple cubic structure—(1st intersects 2nd) means valleys due to 1st NN interaction intersecting valleys due to 2nd NN interaction yield cusps (011) and (001). Underlined index refers to the first time this index has appeared.

TABLE I, PART 1 (*continued*)

Structure	Nearest Neighbor Interaction	Spherical Polygon	σ_{hkl} Multiplied by $a^2(h^2+k^2+l^2)^{1/2}$	Equilibrium Planes in Order of Their Appearance
face centered cubic	1st	(001, 111, 1$\bar{1}$1)	$4(k+2l)$	
	2nd	(001, 010, 100)	$4(h+k+l)$	
	3rd	(001, 012, 113, 102)	321	
		(113, 135, 111, 315)	$12(h+k+2l)$	
		(102, 315, 101, 3$\bar{1}$5)	$8(2h+3l)$	
		(315, 111, 101)	$4(5h+2k+5l)$	
		(102, 113, 315)	$4(2h+k+7l)$	

*	1st	2nd	3rd
1st	001 111	011 001	113 011 111
2nd		001	012 111 011
3rd			135 111 011 113 012

Structure	Nearest Neighbor Interaction	Spherical Polygon	σ_{hkl} Multiplied by $a^2(h^2+k^2+l^2)^{1/2}$	Equilibrium Planes in Order of Their Appearance
body centered cubic	1st	(101, 011, $\bar{1}$01, 0$\bar{1}$1)	$4l$	
		(101, 011, 110)	$2(h+k+l)$	
	2nd	(001, 010, 100)	$2(h+k+l)$	
	3rd	(001, 111, 1$\bar{1}$1)	$4(k+2l)$	

*	1st	2nd	3rd
1st	011	011	112 011
2nd		001	001 011
3rd			111 001

Structure	Nearest Neighbor Interaction	Spherical Polygon	σ_{hkl} Multiplied by $a^2(h^2+k^2+l^2)^{1/2}$	Equilibrium Planes in Order of Their Appearance
cubic diamond	1st	(111, $\bar{1}$11, $\bar{1}\bar{1}$1, 1$\bar{1}$1)	$4l$	
	2nd	(001, 111, 1$\bar{1}$1)	$8(k+2l)$	
	3rd	(113, $\bar{1}$13, $\bar{1}\bar{1}$3, 1$\bar{1}$3)	$20l$	
		(113, 1$\bar{1}$3, 101)	$4(3h+4l)$	
		(101, 113, 111)	$4(4h+2k+3l)$	

*	1st	2nd	3rd
1st	111	111	011 111
2nd		061 111	113 111 011
3rd			113 111 011

TABLE I, PART 2

Structure	Nearest Neighbor Interaction	Spherical Polygon	σ_{hkl} Multiplied by $ac(h^2+k^2+(a/c)^2l^2)^{1/2}$	Equilibrium Planes in Order of Their Appearance
beta tin	1st	$(101, 011, \bar{1}01, 0\bar{1}1)$	$2l$	
		$(011, 101, 10\bar{1}, 01\bar{1})$	$2(h+k)$	
	2nd	$(100, 010, \bar{1}00, 0\bar{1}0)$	$4l$	
	3rd	$(101, 011, \bar{1}01, 0\bar{1}1)$	$6l$	
		$(101, 011, 010, 100)$	$2(h+k+2l)$	

*	1st	2nd	3rd
1st	011	010	011 010
2nd		none	010
3rd			011 010

Structure	Nearest Neighbor Interaction	Spherical Polygon	σ_{hkl} Multiplied by $ac(h^2+k^2+hk+\frac{3}{4}(a/c)^2l^2)^{1/2}$†	Equilibrium Planes in Order of Their Appearance
hexagonal close packed	1st	$(0001, 10\bar{1}1, 01\bar{1}1)$	$4h+4k+3l$	
		$(10\bar{1}1, 01\bar{1}1, 01\bar{1}0, 10\bar{1}0)$	$6h+6k+l$	
	2nd	$(10\bar{1}2, 01\bar{1}2, \bar{1}102, \bar{1}012, 0\bar{1}12, 1\bar{1}02)$	$3l$	
		$(10\bar{1}2, 01\bar{1}2, 01\bar{1}1, 11\bar{2}0, 10\bar{1}1)$	$4h+4k+l$	
		$(10\bar{1}1, 11\bar{2}0, 10\bar{1}0)$	$6h+2k-l$	
	3rd	$(l \geq 0)$	$2l$	

*	1st	2nd	3rd
1st	$\underline{0001}$ $\underline{10\bar{1}1}$ $\underline{10\bar{1}0}$	$\underline{10\bar{1}2}$ $\underline{11\bar{2}0}$ $\underline{10\bar{1}1}$ $10\bar{1}0$	1010
2nd		$10\bar{1}2$ $10\bar{1}1$ $11\bar{2}0$	$10\bar{1}0$ $11\bar{2}0$
3rd			none

TABLE I, PART 2 (*continued*)

Structure	Nearest Neighbor Interaction	Spherical Polygon	σ_{hkl} Multiplied by $ac(h^2+k^2+(a/c)^2l^2)^{1/2}$	Equilibrium Planes in Order of Their Appearance
"hexagonal diamond" (wurtzite type)	1st	$(0001, 10\bar{1}0, 01\bar{1}0)$	$2h+2k+l$	
	2nd	$(0001, 10\bar{1}1, 01\bar{1}1)$ $(10\bar{1}1, 10\bar{1}0, 01\bar{1}0, 01\bar{1}1)$	$2(4h+4k+3l)$ $2(6h+6k+l)$	
	3rd	$(10\bar{1}2, 11\bar{2}0, 01\bar{1}2, \bar{1}2\bar{1}0$, etc.) $(10\bar{1}2, 11\bar{2}0, 10\bar{1}1)$ $(10\bar{1}1, 11\bar{2}0, 2\bar{1}\bar{1}0)$	l $2(h-k)$ $2l$	

*	1st	2nd	3rd
1st	0$\underline{\bar{1}}$01 1$\underline{\bar{1}}$0	1$\underline{\bar{1}}$1 0001 10$\bar{1}$0	10$\underline{\bar{1}}$2 11$\underline{\bar{2}}$0 10$\bar{1}$1
2nd		0001 10$\bar{1}$0 10$\bar{1}$1	10$\bar{1}$2 11$\bar{2}$0 10$\bar{1}$1
3rd			11$\bar{2}$0

* Intersects; *i.e.*, in simple cubic structure—(1st intersects 2nd) means valleys due to 1st NN interaction intersecting valleys due to 2nd NN interaction yield cusps (011) and (001). Underlined index refers to the first time this index has appeared.

† Since the energies of the nearest neighbor bonds within the (0001) layer and normal to it are assumed to be identical, the values given apply only to a value of $c/a=(8/3)^{1/2}$.

If the values of the energies of these bonds within the (0001) layer, E_a, and normal to it, E_c, are not equal, then $c/a \neq (8/3)^{1/2}$ and the specific surface energy values for the various planes are changed. This results in a modification of the crystal forms as a function of $P=E_c/E_a$. It is to be expected that $P<1$, and E_a=NN interaction energy. For hexagonal close packing, for example, for any given c/a ratio, the surface energy values of the spherical triangle and quadrangle change from the above expressions to $4(h+k)+3Pl$ and $2(2+P)(h+k)+Pl$, respectively. Here, with varying P, the crystal form changes only its ratio of axial to radial dimension; for hexagonal diamond structure, however, the crystal form abruptly changes with the appearance and disappearance of specific planes at the critical values $P=1$ and $P=3$.

TABLE I, PART 3

Structure Type	Bond Energy Ratio	Nearest Neighbor Interaction	Spherical Polygon	σ_{hkl} Multiplied by $ac(h^2+k^2+hk+3/4(a/c)^2l^2)^{1/2}$	Equilibrium Planes in Order of Their Appearance
selenium	$R\leq\frac{1}{2}$	1st & 2nd	$(10\bar{1}1, \bar{1}101, 0\bar{1}11)$ $(10\bar{1}1, 01\bar{1}0, \bar{1}101)$ $(10\bar{1}1, 10\bar{1}0, 01\bar{1}0)$	$(1+2R)l$ $2Rh+4Rk+l$ $4Rh+4Rk+(1-2R)l$	Se; $R<\frac{1}{2}$
	$R\geq\frac{1}{2}$	1st & 2nd	$(10\bar{1}1, \bar{1}101, 0\bar{1}11)$ $(10\bar{1}1, 01\bar{1}0, \bar{1}101)$ $(10\bar{1}1, 01\bar{1}\bar{1}, 10\bar{1}0)$	$(1+2R)l$ $2Rh+4Rk+l$ $4Rh+2k+(1-2R)l$	
	$R\leq\frac{1}{2}$†	3rd Se; 4th Te	$(\ldots\geq 0)$	$2l$	
	$R\geq\frac{1}{2}$†	3rd Se; 4th Te	$(0001, 10\bar{1}1, 01\bar{1}0, \bar{1}101, 0001)$ $(10\bar{1}1, 11\bar{2}0, 01\bar{1}0)$ $(10\bar{1}1, 10\bar{1}0, 11\bar{2}0)$	$2l$ $2h$ $2(k+l)$	
	$R>0$	4th Se; 3rd Te	$(0001, 10\bar{1}0, 000\bar{1}, 01\bar{1}0, 0001)$	$6(h+k)$	

Se; $R<\frac{1}{2}$

*	1st	1st & 2nd	3rd	4th
1st	none	$\underline{10\bar{1}0}$	none	$10\bar{1}0$
1st & 2nd		$\underline{10\bar{1}1}$ $10\bar{1}0$	$10\bar{1}0$	$10\bar{1}1$ $10\bar{1}0$ $\underline{10\bar{1}2}$
3rd			none	$10\bar{1}0$
4th				$\underline{00C1}$

Se; $R>\frac{1}{2}$

*	1st & 2nd	3rd	4th
1st & 2nd	$\underline{10\bar{1}1}$ $\underline{10\bar{1}0}$	$10\bar{1}1$ $10\bar{1}0$ $\underline{11\bar{2}C}$	$10\bar{1}1$ $10\bar{1}0$ $\underline{10\bar{1}2}$
3rd		$10\bar{1}1$ $10\bar{1}0$	$10\bar{1}1$ $10\bar{1}0$
4th			$\underline{0001}$

* Intersects; e.g., in simple cubic structure—(1st intersects 2nd) means valleys due to 1st NN interaction intersecting valleys due to 2nd NN interaction yield cusps ($\underline{C11}$) and (001). Underlined index refers to the first time this index has appeared.

† It is assumed that 3rd and 4th nearest neighbor interactions are negligible as compared to 1st and 2nd nearest neighbor interactions and that, therefore, the surface structure of the various planes as derived from 1st and 2nd nearest neighbor interaction remains unchanged.

TABLE I, PART 3 (*continued*)

Structure Type	Bond Energy Ratio	Nearest Neighbor Interaction	Spherical Polygon	σ_{hkl} Multiplied by $ac(h^2+k^2+hk+3/4(a/c)^2l^2)^{1/2}$	Equilibrium Planes in Order of Their Appearance
arsenic	$R \leq \frac{1}{3}$	1st & 2nd	$(0001, 01\bar{1}2, \bar{1}101)$ $(01\bar{1}2, \bar{1}101, \bar{1}10\bar{2})$	$3(-2Rh+(1-R)k+Rl)$ $-4Rh+(R+3)k+Rl$	As; $R \leq \frac{1}{3}$
	$R \geq \frac{1}{3}$	1st & 2nd	$(0001, 01\bar{1}2, \bar{1}012)$ $(01\bar{1}2, \bar{1}101, \bar{1}012)$ $(01\bar{1}2, \bar{1}101, \bar{1}10\bar{2})$	$3((R-1)h+(1-R)k+Rl)$ $-(3R+1)h+(3R+1)k+l$ $-4Rh+(R+3)k+Rl$	As; $R > \frac{1}{3}$
	$R > 0$	3rd	$(0001, 01\bar{1}0, 000\bar{1}, \bar{1}100, 0001)$	$12k$	

As; $R \leq \frac{1}{3}$

*	1st	1st & 2nd	3rd
1st	0001	$01\bar{1}2$ $01\bar{1}\bar{1}$	0001
1st & 2nd		$01\bar{1}2$ $01\bar{1}\bar{1}$	$01\bar{1}2$ $01\bar{1}\bar{1}$
3rd			0001

As; $R > \frac{1}{3}$

*	1st	1st & 2nd	3rd
1st	0001	$01\bar{1}2$ $01\bar{1}\bar{1}$	0001
1st & 2nd		$01\bar{1}2$ $01\bar{1}\bar{1}$	$01\bar{1}2$ $01\bar{1}\bar{1}$ $01\bar{1}4$
3rd			0001

$$R = \frac{\text{2nd nearest neighbor bond energy}}{\text{1st nearest neighbor bond energy}}$$

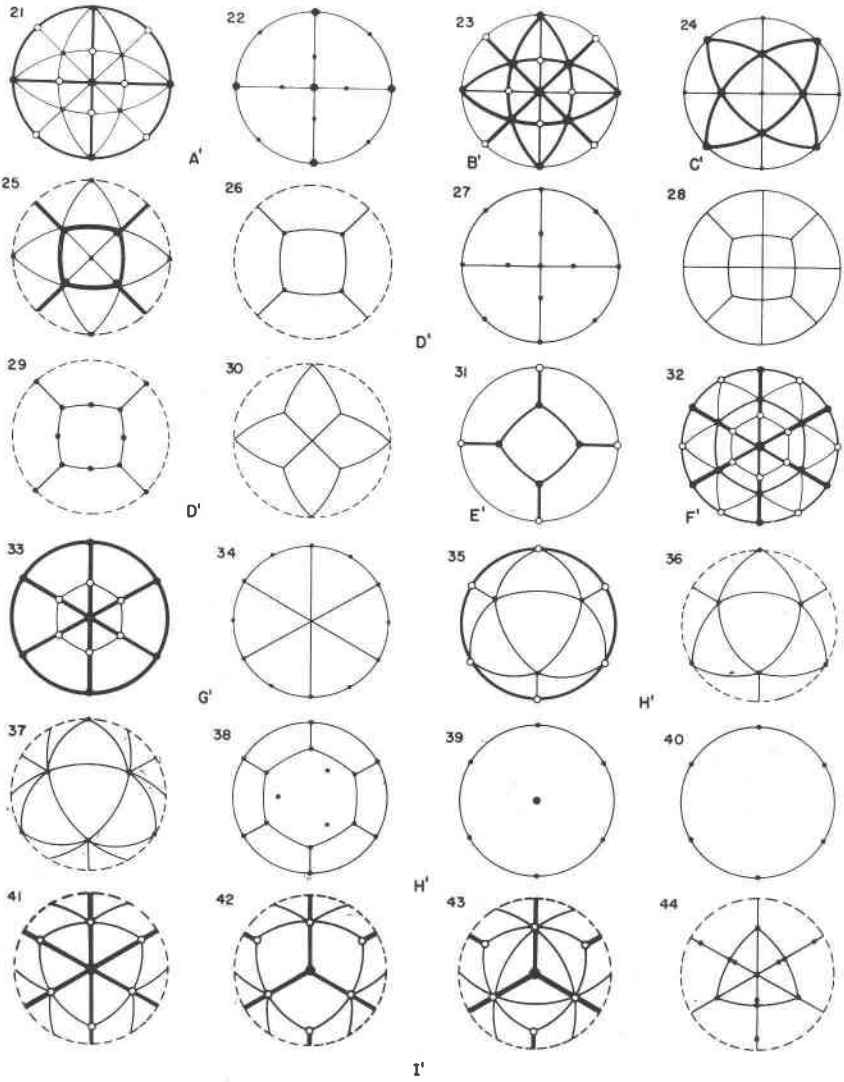

FIG. 4. Nos. 21–44. Stereograms of equilibrium forms, microcleavage patterns, and thermal etch patterns. In stereograms of equilibrium forms, heavy lines represent crystal zones (or crystal edges) as a result of 1st NN interaction only. Light lines correspond to zones as a result of 2nd NN interaction only. Large filled circles represent cusps due to 1st NN valleys intersecting each other. Small filled circles represent cusps due to 2nd NN valleys intersecting each other; and large open circles represent cusps due to 1st NN valleys intersecting 2nd NN valleys.

Filled circles in all other stereograms represent planes with their degree of development indicated by the size of the circles. Lines represent zones, and dashed lines are used only to

librium planes for all structures investigated are to be found in Fig. 4. Figure 1 gives two examples of three-dimensional Wulff's plots with their corresponding PBC vectors.

Discussion of Wulff's Plots, Habit, and PBC Vectors, Microcleavage and Activation Energy of Nucleation

In evaluating Wulff's plots it is useful to correlate the crystallographic zones to the corresponding strong bonding arrays or PBC vectors (Hartman and Perdok, 1955). These zones may be found by a microcleavage (Wolff and Broder, 1959; Wolff, 1962) or habit study. The three-dimensional Wulff's plots (Fig. 1) exhibit maxima, valleys and cusps. Where the valleys (Kleber, 1959) include an angle of 360° (Fig. 1) the atoms lie either along one straight array ([001] in s.c.) or are composed of double or triple zig zag arrays ([001] in rutile and marcasite structures, or [001] in wurtzite and h.c.p., respectively). Any other zig zag array or PBC vector of this type results in a valley and includes an angle of less than 360°. This is also true for a PBC vector composed of two vectors of different strengths (E_1, E_2), *e.g.*, in As and Se. In cases such as these, at some critical ratio of the strengths of the two vectors ($E_2/E_1 = \frac{1}{3}$ for As and $E_2/E_1 = \frac{1}{2}$ for Se), one type of valley disappears to be replaced by another type. A very good approximation of the ratio of the bond strengths is arrived at by comparing these theoretically derived habits with those observed on natural, synthetic or microcleaved crystals. For example, the three forms of this type are shown for As, Sb and Bi in Fig. 3, Nos. 18, 19 and 20, respectively, and for Se and Te in Fig. 3, No. 15 (Dana, 1920, 1951).

There are certain cases where experimentally observed and theoretically calculated crystal forms are not identical. In this case, valleys in the Wulff's plot of these crystals exist for the experimental form but do not exist in the derived form and, in some cases, valleys do not exist for the experimental form where they do exist for the derived form. These valleys

---

indicate the outline of the stereograms.

21) s.c. equilibrium form. 22) NaCl microcleavage. 23) f.c.c. equilibrium form. 24) b.c.c. equilibrium form. 25) diamond equilibrium form. 26) diamond microcleavage. 27) HgTe microcleavage. 28) $AuGa_2$ microcleavage. 29) InSb microcleavage. 30) α—Sn microcleavage. 31) β—Sn equilibrium form. 32) h.c.p. equilibrium form. 33) wurtzite equilibrium form. 34) Cds microcleavage. 35) Se, $E_\beta < \frac{1}{2} E_\alpha$ equilibrium form. 36) Se, $E_\beta = \frac{1}{2} E_\alpha$, equilibrium form. 37) Se, $E_\beta > \frac{1}{2} E_\alpha$, equilibrium form. 38) Te thermally etched at 350° for three hours. 39) Te microcleavage. 40) HgS (cinnabar) microcleavage. 41) As, $E_\beta < \frac{1}{3} E_\alpha$, equilibrium form. 42) As, $E_\beta = \frac{1}{3} E_\alpha$ equilibrium form. 43) As, $E_\beta > \frac{1}{3} E_\alpha$ equilibrium form. 44) Sb thermally etched at 600° C. for six hours. Attention is called to the zones (lines) connecting two planes (filled circles) which correspond to the edge joining the two planes. The lines also correspond to PBC vectors. Light lines are not shown wherever heavy lines appear.

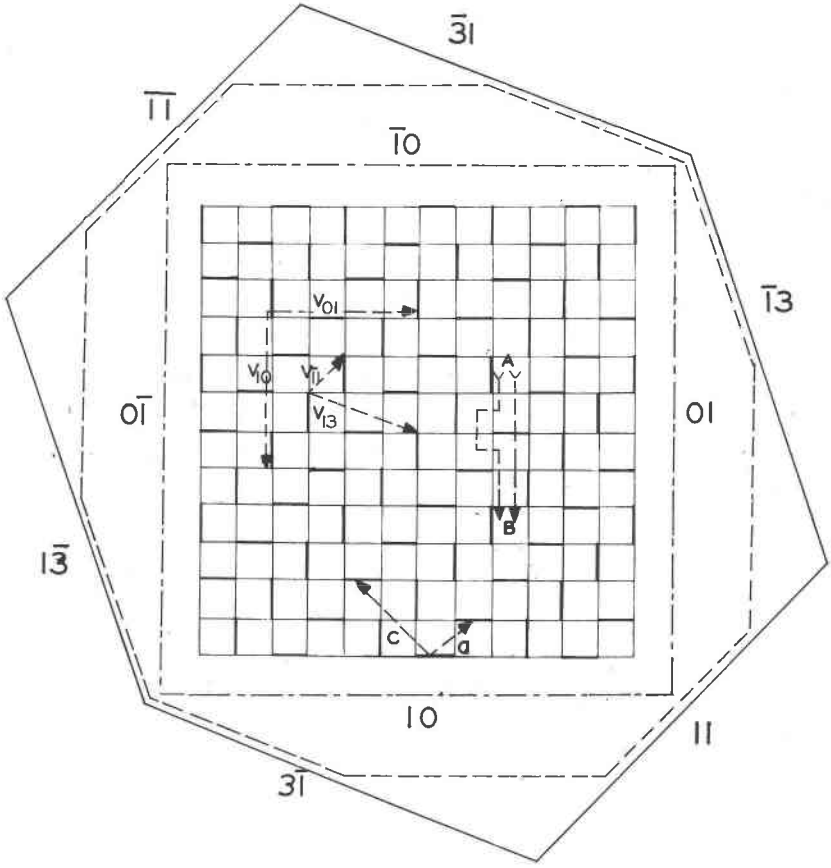

FIG. 5. A two-dimensional representation of the I_2 or Br_2 type structure in the b or (010) plane. The direction follows c and a as indicated. Strong bonds are represented as heavy lines; weak bonds are represented as light lines. The bonds above and below the plane are not considered. They correspond to close-packing. It should be noted that the straight vector AB represents the least energetic mode of bond separation when the heavily drawn bonds are as strong as the light bonds. In this case, a square results as an equilibrium form in two dimensions. The identical vectors V_{01} and V_{10} then prevail. When the heavily drawn bonds are more than three times stronger than the weak bonds, the two vectors V_{11} and V_{13} then prevail. It is obvious that a vector of the type V_{10} in the direction of AB will circumvent the strong bond and cut the three neighboring weak bonds which, together, are weaker than the strong bond. Thus, in this case V_{11} and V_{13} holds for $R<\frac{1}{3}$. R represents the bond strength ratio E_β/E_α. For $R<\frac{1}{3}$ ($\bar{1}3$) and (11) prevail; for $1>R>\frac{1}{3}$ ($\bar{1}3$), (11), (01), and (10) are observed; and for $R=1$ there are only (01) and (10) outlines. In this discussion, bondings above and below the plane are not considered.

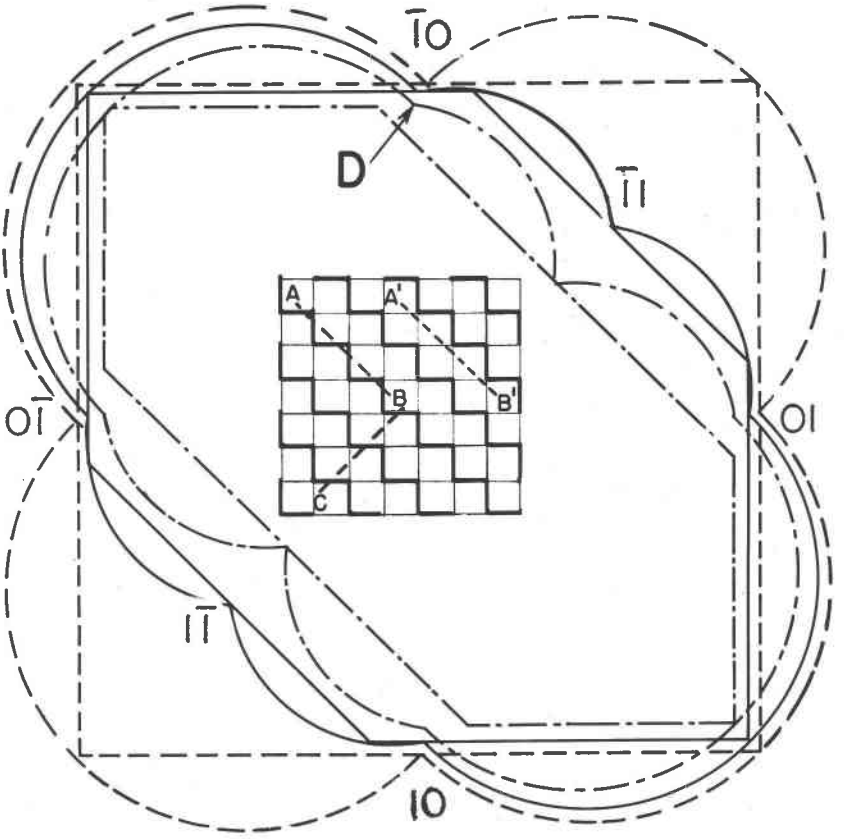

FIG. 6. As-type structure; $(10\bar{1}1)$ plane. The bonds above and below the plane of projection are not considered. Two types of bonds are present, strong bonds (heavy lines) and weak bonds (light lines). Two typical types of cuts, parallel to $(\bar{1}1)$, AB or A′B′ are possible. AB cuts only strong bonds, When $E_\beta = E_\alpha$, *i.e.* the strengths of the bonds are equal, it would make no difference cutting BC, AB or A′B′. The resulting habit in this case is a square. For $E_\beta < E_\alpha$ a truncation of type $(\bar{1}1)$ appears.

(and their associated PBC vectors) result from the absorption of foreign atoms onto the crystal surface and/or from the displacement of surface atoms into energetically more favorable positions. Such changes, although quite negligible for close packed metals and Van der Waals type crystals, are rather common in covalent type crystals.

It is possible from a habit study to determine fairly precisely the positions of the displaced and/or absorbed atoms. The diamond structure, for instance, presents a good example. In this structure the surface atoms

lack either one or two neighbor atoms. This results in "dangling" bonds. For the planes $l \geq h \geq k$, the number of single "dangling" bonds (denoted by s) per unit area as a function of h, k and l is $4h$ and that of the double "dangling" bonds (denoted by d) is $-4h+4l$. Bivalent foreign atoms absorbing to the surface will generally bond only to surface atoms with two "dangling" bonds. Upon absorption the surface energy per bond E_s (referring now to what were previously "dangling" bonds) will be lowered to a new value E_d. This is equivalent to $\alpha = (E_s - E_d)/E_s$ where α is the relative amount by which the surface energy per bond was lowered. The specific surface energy in this case will be given by $\sigma_{hkl} = sE_s + dE_d$ per planar cell area or by $(4[\alpha h + (1-\alpha)l]E_s)/a_0^2(h^2+k^2+l^2)^{\frac{1}{2}}$. For small values of $\alpha(\alpha < \frac{1}{2})$ (001) appears in addition to (111) and two PBC vectors, [110] and $[1\bar{1}0]$, (both associated with the appearance of (001)) come into existence.

Critical Bonding Ratio

An investigation has been made of crystal habit of the elements Se, Te, Po, Sn, As, Sb, Bi, Br_2 and I_2. All exhibit a bonding which could be described as mixed sp^3 and p^3 bonding. The atoms of Vb and VIb elements are in a nearly octahedral arrangement, surrounded respectively by 3+3 and 2+4 nearest and next-nearest neighbors. In simple cubic Po, which has a 6-fold coordination, there is no difference between nearest and next-nearest neighbors. In arsenic type structures the theoretical habit is shown in Fig. 3, Nos. 18, 19, 20. Here, the interaction between next-nearest neighbors is less than $\frac{1}{3}$, equal to $\frac{1}{3}$ and greater than $\frac{1}{3}$, respectively, of the interaction between nearest neighbors. In this case the habit changes from tabular to pseudo-cubic (For comparison with natural habit, see Dana, 1951). The theoretical habit for the selenium type structure is given in Nos. 15, 16, and 17 of Fig. 3. The interaction between next-nearest neighbors is less than $\frac{1}{2}$, equal to $\frac{1}{2}$, and greater than $\frac{1}{2}$ of that between nearest neighbors, respectively. As a result, the habit changes from hexagonal prismatic to pseudocubic.

To illustrate this principle of critical bonding ratio, consider a crystal of only two dimensions as shown in Fig. 5. It is seen that (11) and $(\bar{1}3)$ are the lines (two-dimensional "planes") with the lowest "specific outline free energy," *i.e.* the two dimensional "specific surface free energy." (Wulff's two-dimensional plots and crystals are enclosed.) The crystal habit corresponding to the outermost "habit" outline is observed only when the bond energy between next-nearest neighbors E_2 is less than or equal to one-third the bond energy between nearest neighbors E_1. When the ratio E_2/E_1 is greater than the critical value $\frac{1}{3}$, it is obvious that the habit changes. In Case 1 with $E_2/E_1 \leq \frac{1}{3}$, only the PBC vectors $V_{\bar{1}1}$ and

V_{13} exist (outermost "habit" outline); in Case 2, with $1 > E_2/E_1 > \frac{1}{3}$, the two equivalent vectors V_{01} and V_{10} also exist (intermediate "habit" outline). In Case 3, with $E_2/E_1 = 1$, only V_{01} and V_{10} exist (innermost square "habit" outline). In each case, the following habits are derived:

Case 1) {11} and $\{1\bar{3}\}$ are present. Vectors $V_{\bar{1}1}$ and V_{13} are parallel to the corresponding outline of the two-dimensional crystal.

Case 2) {11}, $\{1\bar{3}\}$ and {01} are present. With increasing E_2/E_1, {01} increases in size as compared to {11} and {13}.

Case 3) The last two outlines disappear when $E_1 = E_2$ (or $E_2/E_1 = 1$) and only {01} is found. The symmetry obtained is now quadratic and shows (Fig. 5) the cross section (100) of a crystal with simple cubic structure.

In this connection it should be noted that the crystal illustrated in Fig. 5 can be cut in two ways between A and B. Either six bonds between next-nearest neighbors (vectors V_2) are cut or three bonds between next-nearest neighbors and one bond (vector V_1) between nearest neighbors are cut. If the former is true ($E_2/E_1 \leq \frac{1}{3}$), the strong V_1 bond is circumvented by cutting the three weak V_2 bonds next to V_1. Should the latter be true, $1 \geq E_2/E_1 > \frac{1}{3}$. Then less energy is expended when V_1 is cut in the process. Consequently, V_{10} is established as the new PBC vector.

There are two more examples, enargite and chalcopyrite, which may be used to demonstrate the estimation of the bond strength ratio which is obtained by comparing habits which have been theoretically and experimentally derived. The experimentally determined microcleavage habit is used in these examples. The advantage of this method of determining habit is that a unique form results, that is, there is only one such habit for each material (Wolff and Broder, 1960). While there is a disadvantage to this method in the neglect of hemihedral properties, conclusions drawn concerning bond strengths within the bulk of the crystal are unaffected.

For enargite a bond ratio estimate of three between the As—S bond and the Cu—S bond results, giving good agreement between the theoretical and microcleavage habit. For chalcopyrite the bond strength ratio between Fe—S and Cu—S (or vice versa) is at least two (or $\frac{1}{2}$). For symmetry reasons it is not possible to decide which bond is stronger.

Discussion of Hemihedrism

Most experimental or theoretical determinations of σ_{hkl} consider only the energy of separation parallel to the plane (*hkl*). What is found is the sum of surface energies of the two new planes. The specific surface energy, however, of each plane remains obscure. The usual procedure is to divide the total surface energy by two so as to assign a surface energy

to each plane; but, as previously mentioned, this holds only when the new planes possess identical structure. That this is, indeed, true may be drawn from conclusions made from habit studies. For example, the tetrahedral habit of sphalerite (ZnS) shows the negative $(\bar{1}\bar{1}\bar{1})$ plane to be more developed than its positive (111) counterpart. This indicates that the negative $(\bar{1}\bar{1}\bar{1})$ plane is the more stable plane. It, therefore, in accordance with Wulff's law has a lower specific surface energy.

The differences in the two planes can be described in terms of the differences in rearrangement of atoms, chemical bonds, and bonding orbitals of the atoms in their surfaces. For example, in sphalerite the two new planes would have zinc atoms on (111) and sulfur atoms on $(\bar{1}\bar{1}\bar{1})$. Since in the bulk sulfur has **ca.** 7 electrons and zinc **ca.** 1 (Wolff and Broder, 1959), it is very probable that the sulfur $(\bar{1}\bar{1}\bar{1})$ electronic configuration would be more stable by virtue of its extra electrons with respect to tetrahedral bonding. The conclusion arrived at is that for materials lacking a center of symmetry the "anionic" plane is more stable. Habit studies, in confirmation of this, indicate a more highly developed "anionic" plane. A difference in the two planes appears also in the III-V compounds and in etching experiments.

Assuming a surface energy assigned to the different surface atoms as denoted by $(A)_s$, $(A)_d$, $(C)_s$, and $(C)_d$ for anionic and cationic single and double "dangling" bonds, then the σ_{hkl} formula for sphalerite structure materials is

$$\sigma_{hkl} = \frac{2[(A)_s - 2(A)_d + (C)_s]h + 2[(A)_s - (C)_s]k + 4(A)_d l}{a_0^2(h^2 + k^2 + l^2)^{1/2}}$$

When $(A)_s = (A)_d \equiv (A)$, $(C)_s \equiv (C)$, and $(C)/_{(A)} = \beta \geq 3$,

$$\sigma_{hkl} = \frac{[2(\beta - 1)(h - k) + 4l](A)}{a_0^2(h^2 + k^2 + l^2)^{1/2}}$$

and a tetrahedron with only tetrahedral "anionic" planes appears. For many materials of this structure type (GaP, ZnS and others) (111), $(\bar{1}\bar{1}\bar{1})$ and (001) are observed. This can easily be explained when $(A)_d/(A)_s < 1$. This is illustrated in Fig. 7. In this way, therefore, it is possible to investigate the bonding structure of the surface atoms.

Ionic Crystals

Most arguments which have been set forth thus far may correctly be applied only to elements, *i.e.*, to materials with Van der Waals, metallic or covalent bonding. In this case, the bonding and electron distribution between the atoms is symmetrical and the interaction energy between the atoms falls off rapidly with interatomic distance. As a rule, however, compounds differ from elements in that the electron distribution of the bonding is asymmetrical. This is due to the partial ionic character of the

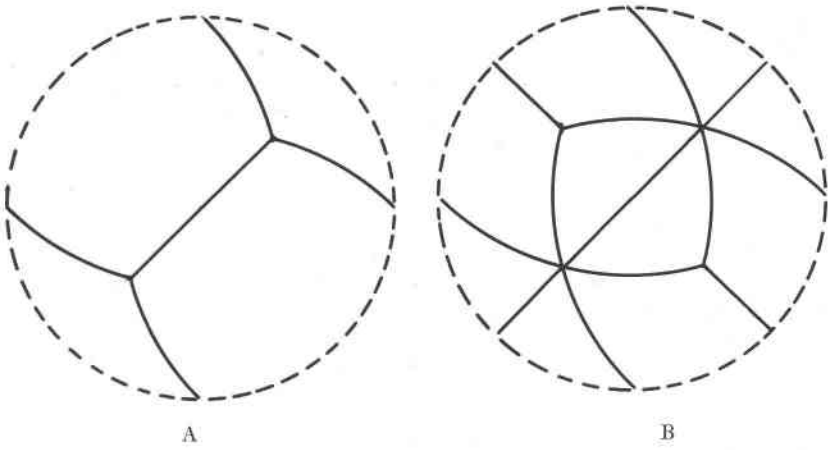

FIG. 7. Stereograms representing equilibrium forms of crystals having sphalerite structure. A) a negative tetrahedron $(1\bar{1}1)$ exists when $\sigma_{111}/\sigma_{1\bar{1}1}=\beta\geq 3$; B) a negative tetrahedron $(1\bar{1}1)$ with minor development of the positive tetrahedron (111) for $3>\beta>1$. C) major $(1\bar{1}1)$, minor (111), (001); not shown here. This form is quite common and appears when the atoms with two "dangling" bonds move to more favorable surface positions or rearrange their electronic structure.

bonding in which there is an attractive force exerted by first nearest and other neighbor atoms as well as a repulsive force exerted by still other neighbors.

For crystals with Van der Waals, metallic and covalent bonding the interaction energy between atoms decreases with r^{-n} where $n=6$ and r is the interatomic distance. For electrostatic bonding, on the other hand, $n=1$. In this type of bonding it appears that the interaction energy of more distant atoms should still be considered while, for all practical purposes, in the former type only up to next-nearest neighbors need to be considered. This renders the calculation of the surface energy and the equilibrium form for ionic crystals extremely difficult by the method outlined here. Sufficient experimental agreement has been found, however, between the calculated equilibrium forms and observed microcleavage forms to justify, in a first approximation, the validity and usefullness of the principles cited herein. This agreement is probably due to the partial ionic character of most compounds and also probably to the screening effect of nearer ions on the interaction on more distant ions.

To take into account the ionic nature of compounds, the specific surface free energy may be approximated by a formula of the type

$$\sigma_{hkl} = (\sigma_{\mathrm{I}} + \mathrm{a}\sigma_{\mathrm{II}} + \mathrm{b}\sigma_{\mathrm{III}} + \mathrm{c}\sigma_{\mathrm{IV}})hkl$$

where a, b, and c are constants and I, II, III, IV refer to 1st, 2nd, 3rd, and 4th nearest neighbor interactions.

Acknowledgments

The authors wish to express their thanks to Drs. A. A. Giardini, J. A. Kohn, F. W. Leonhard and to Mr. J. Hietanen for interesting discussions and constructive criticism of the manuscript.

References

Buerger, M. J. (1947) The relative importance of the several faces of a crystal, *Am. Mineral.*, **32,** 593–606.

Burton, W. K. and Cabrera (1949) Crystal growth and surface structure, *Disc. Faraday Soc.* **5,** 33–39.

Dana, J. D. (1951) The System of Mineralogy, John Wiley and Sons, New York.

Donnay, J. D. H. and D. Harker (1937) A new law of crystal morphology extending the law of Bravais, *Am. Mineral.*, **22,** 446–467.

Gibbs, J. W. (1928) Collected Works, Longman Green and Co., New York.

Hartman, P. (1959) The effect of adsorption on the face development of the equilibrium form, *Acta Cryst.*, **12,** 429–439.

——— (1958) The equilibrium forms of crystals, *Acta Cryst.*, **11,** 459–464.

——— and W. G. Perdok, (1955) On the relations between structure and morphology crystals, *Acta Cryst.*, **8,** 49–52, 521–529.

Herring, C. (1950) Some simple theorems on the free energies of crystal surfaces, *Phys. Rev.*, **75,** 344–350.

Honigmann, B. (1959) Gleichgewichts- und Wachstumformen von Kristallen, *Fort. phys. Chemie,* Dr. Dietrich Steinkopff Verlag, Darmstadt.

Kern, R. and J. C. Monier (1956) Interprétation des formes caractéristiques de cristaux appartenant aux mériédries non centrées, *Bull. Soc. Franç. Min.* **78,** 461.

Kleber, W. (1937) Die Struktur theoretische Diskussion kristall-morphologischer Fragen, *Fort. Min.*, **21,** 169–224.

——— (1957) Über flächenspezifische Adsorption und Solvation, *Zeit. phys. Chem.*, **206,** 327–338.

Kossel, W. (1928) Die molekularen Vorgänge beim Kristallwachstum, Leipziger Vortraege, Hirzel, Leipzig, pp. 1–46.

Stranski, I. N. (1956) Propriétés des surfaces des cristaux, *Bull. Soc. Franç. Min.* **79,** 359–383.

——— (1928) Zur Theorie des Kristallwachstums, *Zeit. phys. Chem.*, (A) **136,** 259–278.

——— and B. Honigmann (1950) Die spontane Einstellung von Gleichgewichtsformen an Hexamethylentetraminkristallen, *Zeit. phys. Chem.*, **194,** 180–198.

——— and R. Kaishev (1935) Crystal growth and formation of nuclei, *Phys. Zeit.* **36,** 393–403.

Wells, A. F. (1946) Crystal habit and internal structure, *Phil. Mag.*, **37,** 184–199; 217–236; 605–630.

Wolff, G. A. (1962) Zum Problem der Gleichgewichtsformen von Kristallen. *Zeit. phys. Chem.* (N.F.) **31,** 1–22.

——— and J. D. Broder (1959) Microcleavage, bonding character and surface structure in materials with tetrahedral coordination, *Acta Cryst.*, **12,** 313–323.

——— (1960) Cleavage and the identification of minerals. *Am. Mineral.* **45,** 1230–1242.

Wulff, G. (1901) Zur Frage der Geschwindigkeit des Wachstums und der Auflösung der Kristallflächen, *Zeit. Krist.*, **34,** 449–530.

Yamada, M. (1924) Über die Kristallformen und die Kristallgitter, *Phys. Zeit.*, **25,** 289–296.

Manuscript received, May 20, 1960.